Published in final edited form as:
Circulation. 2014 September 9; 130(11 0 1): S77–S86. doi:10.1161/CIRCULATIONAHA.113.007920.

Cardiac Tissue Slice Transplantation as a Model to Assess Tissue-Engineered Graft Thickness, Survival, and Function

Johannes Riegler, PhD, **Astrid Gillich, PhD**, **Qi Shen, MS**, **Joseph D. Gold, PhD**, and **Joseph C. Wu, MD, PhD**
Department of Medicine, Division of Cardiology and Department of Radiology, Stanford Cardiovascular Institute (J.R., Q.S., J.C.W.), Department of Biochemistry (A.G.), and Department of Cardiothoracic Surgery (J.D.G.), Stanford University School of Medicine, CA

Abstract

Background—Cell therapies offer the potential to improve cardiac function after myocardial infarction. Although injection of single-cell suspensions has proven safe, cell retention and survival rates are low. Tissue-engineered grafts allow cell delivery with minimal initial cell loss and mechanical support to the heart. However, graft performance cannot be easily compared, and optimal construct thickness, vascularization, and survival kinetics are unknown.

Methods and Results—Cardiac tissue slices (CTS) were generated by sectioning mouse hearts (n=40) expressing firefly luciferase and green fluorescent protein into slices of defined size and thickness using a vibrating blade microtome. Bioluminescence imaging of CTS transplanted onto hearts of immunodeficient mice demonstrated survival of ≤30% of transplanted cells. Cardiac slice perfusion was re-established within 3 days, likely through anastomosis of pre-existing vessels with the host vasculature and invasion of vessels from the host. Immunofluorescence showed a peak in cell death 3 days after transplantation and a gradual decline thereafter. MRI revealed preservation of contractile function and an improved ejection fraction 1 month after transplantation of CTS (28±2% CTS versus 22±2% control; P=0.05). Importantly, this effect was specific to CTS because transplantation of skeletal muscle tissue slices led to faster dilative remodeling and higher animal mortality.

Conclusions—In summary, this is the first study to use CTS as a benchmark to validate and model tissue-engineered graft studies. CTS transplantation improved cell survival, established reperfusion, and enhanced cardiac function after myocardial infarction. These findings also confirm that dilative remodeling can be attenuated by topical transplantation of CTS but not skeletal muscle tissue grafts.

Correspondence to Joseph C. Wu, MD, PhD, Lorry I. Lokey Stem Cell Research Bldg, 265 Campus Dr, Room G1120B, Stanford, CA 94305-5454. joewu@stanford.edu.

Presented at the 2013 American Heart Association meeting in Dallas, TX, November 16–20, 2013.

The online-only Data Supplement is available with this article at http://circ.ahajournals.org/lookup/suppl/doi:10.1161/CIRCULATIONAHA.113.007920/-/DC1.

Disclosures
None.

Europe PMC Funders Author Manuscripts

Keywords

cell transplantation; magnetic resonance imaging; myocardial infarction; tissue engineering

Europe PMC Funders Author Manuscripts

Cardiovascular diseases are the primary cause of death in the industrialized world. Cell therapies delivering single-cell suspensions of autologous skeletal myoblasts, bone marrow cells, or sorted subpopulations into the myocardium or coronary arteries after myocardial infarction (MI) have proven safe but may lack efficacy.[1] This may be due to the limited ability of these cells to survive and convert into fully mature contractile cardiomyocytes. The development of protocols for efficient differentiation of cardiomyocytes from pluripotent stem cells, such as embryonic stem cells (ESCs) and induced pluripotent stem cells (iPSCs), allows the production of large numbers of cells for transplantation.[2] For example, preclinical experiments have demonstrated that injection of ESC-derived cardiomyocytes into infarcted hearts generates stable grafts showing electric coupling with their host.[3] However, typically <1% of injected cells survive for >1 month, limiting the clinical use of this approach.[4,5] Multiple factors such as loss of cell–cell contact, lack of appropriate mitogens, mechanical stress, inflammation, and ischemia likely contribute to cell loss.

Tissue-engineered constructs are a potential alternative to cell injections and offer additional mechanical support to limit dilative remodeling. Numerous approaches have been explored to generate matrix-free cell sheets or 3-dimensional tissue grafts (reviewed by Ye et al[6]), some of which have advanced to clinical trials.[7] Existing literature suggests that functional benefits of tissue-engineered grafts transplanted onto infarcted hearts may range from increased cardiac wall thickness to reduced dilative remodeling.[8-10] However, a major drawback of this approach is the limited scalability because of oxygen diffusion, which can restrict graft thickness to a few hundred micrometres in the absence of a functional vascular network. Although addition of endothelial cells or fibroblasts improves survival,[8,11] the optimal cellular composition of grafts is not known.

To date, systematic analyses have not been undertaken to determine the maximum thickness of such grafts at the time of transplantation or the potential changes of cellular composition after transplantation. Here, we show that cardiac tissue slices (CTS) of defined size and thickness made from uninjured mice are a suitable standard for comparison of tissue-engineered grafts. We assess the survival of CTS transplanted onto normal or infarcted hearts in vivo using bioluminescence imaging (BLI), characterize cell death, CTS composition, and analyze revascularization of CTS by host vessels. Finally, we use cardiac MRI to quantify the effect of CTS transplantation on infarct size and cardiac remodeling in a mouse MI model.

Methods

An expanded Methods section is available in the online-only Data Supplement.

Transgenic and Reporter Mice Used for This Study

Transgenic L2G mice that express green fluorescent protein and firefly luciferase (Fluc) reporter genes under the control of the β-actin promoter were maintained on a Friend Virus B-type (FVB) background.[12] The Cre reporter line Rosa26-tdTomato that labels cells with tdTomato after Cre-mediated recombination,[13] vascular endothelial-cadherin (Cdh5)-Cre transgenic mice,[14] Sox2-Cre transgenic mice,[15] and immunodeficient Nonobese Diabetic/Severe Combined Immunodeficiency (NOD/SCID) mice were obtained from the Jackson Laboratory. All procedures involving animals were approved by the Stanford Institutional Animal Care and Use Committee in accordance with established guidelines for animal care.

Generation of CTS

Adult (8–12 weeks; n=40) L2G mice were anesthetized using isoflurane. Hearts were perfused with ice-cold modified Tyrode solution, excised, embedded in 4% low melting point agarose (Invitrogen, Carlsbad, CA), and placed on ice. The solidified block was mounted on a sample holder and sectioned with a vibratome. Sections with different thicknesses (100–800 μm) were prepared from the left ventricular free wall. To standardize the size of grafts, circular grafts with 3 or 5 mm diameter were punched out of sections using a core sample puncher and stored in modified Tyrode solution until transplantation (Figure 1A). These discs are referred to as CTS. Skeletal muscle tissue slices were made from thigh muscles (vastus lateralis) of transgenic L2G mice using a similar procedure.

MI and CTS Transplantation

MI was induced in NOD/SCID mice by permanent left anterior descending coronary artery ligation under 1.5% to 2% inhaled isoflurane anesthesia. Animals were randomized into experimental groups receiving CTS (n=36), skeletal muscle patches (n=12), or control group receiving no patch (n=12). For experiments involving cardiac assessment via MRI, CTS and skeletal muscle patches with 5 mm diameter and 400 μm thickness were transplanted directly after left anterior descending coronary artery occlusion. CTS and skeletal muscle patches were attached onto the left ventricular free wall with 4 to 5 stitches using 10-0 silk sutures. For patch survival and reperfusion experiments, CTS with a diameter of 3 mm were transplanted onto the left ventricular free wall of noninfarcted mice (n=52; NOD/SCID). Operations were performed by experienced microsurgeons.

Assessment of Endothelial Cell Origin of Reperfused CTS

CTS were transplanted onto noninfarcted hearts of adult VE-cadherin-Cre; Rosa26-tdTomato double-heterozygous mice (n=18; C57BL/6 background). To prevent immune rejection, tacrolimus (Astellas, 5 mg/kg per day) was orally administered every 12 hours.

Survival of Neonatal CTS

Because most tissue-engineered grafts are made of differentiated ESCs or iPSCs that may be immature, we also generated neonatal CTS to model the survival of such cells. Neonatal CTS were derived from 1-day-old L2G pups. Neonatal CTS were transplanted onto the epicardial surface of adult control (n=5) or infarcted (n=5) NOD/SCID mice.

Bioluminescence Imaging

BLI was performed using the Xenogen in vivo Imaging System (Alameda, CA) as previously described.[4,5]

Immunohistochemistry and Histological Methods

Immunofluorescence and histological analyses were performed using standard protocols.

Magnetic Resonance Imaging

Cardiac function and scar size were assessed on day 1 and day 28 after MI induction and CTS transplantation using a 7T MR901 Discovery horizontal bore scanner (Agilent Technologies, Santa Clara, CA).

Statistical Analysis

Results are shown as mean±SEM unless stated otherwise. To test whether a linear relationship between the number of viable cells and the radiance measured by BLI exists, a regression analysis was performed. To verify whether the radiance from 300 μm CTS changed between days 7 and 60, a 2-tailed Wilcoxon rank-sum test was used. To test whether infarct and CTS thickness were significant factors explaining the observed variation in BLI data, a linear mixed-effects model with fixed effects for CTS thickness, time, and MI and random effects for individual mice was used (residuals were tested for normality using a Shapiro–Wilk test). For comparisons of the radiance from specified groups at day 28, a Wilcoxon rank-sum test followed by Bonferroni correction of *P* values (6 multiple comparisons) was used. To illustrate diffusion-limited survival, a linear mixed-effects model with fixed effects for CTS thickness, CTS thickness squared, MI and random effects for individual mice and measurement time points (BLI day 7–28 data) was used. To test whether increasing CTS thickness leads to equivalent increases in BLI signal intensity, a regression analysis was performed. To test whether differences in scar size could be explained by treatment groups, a Kruskal–Wallis test was performed. To assess whether there are any differences in survival between MRI treatment groups, a Kaplan–Meier survival analysis was performed using a log-rank test. To test for differences in cardiac function, a linear mixed-effects model was used with fixed effects for functional parameter, treatment group, time and a random effect for individual mice. If such an effect was found, Wilcoxon rank-sum tests with Bonferroni corrections of *P* values were performed (3 multiple comparisons). Data correlations were tested using a Pearson correlation test. Statistical analysis was performed using R software version 2.8.1.

Results

Cardiac Tissue Slice Transplantation as a Model to Assess Graft Survival

To evaluate whether healthy cardiac tissues transplanted onto the heart wall can survive long-term in vivo, CTS from adult L2G mice were transplanted onto hearts of immunocompromised mice. Cell loss was observed for the first 7 days with no further decline in cell survival thereafter (P=0.68 day 7 versus day 56; Figure 1B and 1C; Figure IA in the online-only Data Supplement). At 2 months, 31±4% of cells from 300-μm-thick CTS

remained viable, which is higher than <1% viability seen with traditional cell injections.[4,5] BLI signal intensity (on a particular day) relative to initial signal intensity was used as a surrogate for viability because a linear relationship between the number of viable cells and signal intensity was found in vitro (intercept: *P*=0.24; slope: *P*=2.6E-11; Figure IB). To investigate whether initial graft survival is limited by oxygen and nutrient diffusion from the host and to determine the maximum graft thickness, CTS with increasing thicknesses were transplanted onto control and infarcted hearts. Increasing graft thickness from 100 to 200 μm led to higher BLI signal intensity on day 28 (*P*=0.03) and similar viability at day 28 (17±2% versus 22±2%; *P*=0.68), but a further increase to 400 or 800 μm did not increase the BLI signal intensity at day 28 (*P*=0.89, *P*=0.57 compared with 200 μm; Figure 1D; Figure IC in the online-only Data Supplement). These results indicate diffusion-limited survival. This pattern was also found for CTS transplanted onto infarcted hearts (Figure 1E), but BLI signal intensity was lower throughout the experiment (*P*=0.005; Figure 1E; Figure ID in the online-only Data Supplement). To further illustrate the differences in patch survival, we focused on the BLI data between day 7 and day 28 and fitted a model with a linear and a quadratic term for patch thickness (Figure IE and IF in the online-only Data Supplement). We found that a patch thickness of ≈400 μm would lead to the highest overall BLI signal intensity, but survival expressed as fraction of initial signal would be highest for 200 μm patch thickness. Cell survival for 100-μm-thick sections was lower than expected. Confocal imaging of CTS kept in Tyrode solution for 4 hours revealed damaged cells along the cutting surfaces from the vibratome and the core sample punch that had lost their cytoplasmic green fluorescent protein (Figure IIA–IID in the online-only Data Supplement). Therefore, cell death caused by sectioning affects a large fraction of cells in thin sections. We further investigated whether the observed survival of adult CTS is specific to the cardiac microenvironment by transplanting CTS onto the back of mice (Figure IIIA and IIIB in the online-only Data Supplement). Similar to the results obtained from transplanting CTS onto the heart, cell loss was observed for the first 7 days, with stable engraftment thereafter preserving 17±7% of transplanted cells for 200 μm CTS thickness. The absolute signal intensity was higher for these CTS because of their close proximity to the skin, leading to reduced tissue absorption and scattering of emitted light compared with the heart that is further away from the skin. Taken together, these results show that a considerable number of cells engraft long-term after CTS transplantation, but initial survival is diffusion limited.

Comparison of Adult With Neonatal CTS Survival

Because most cardiac tissue–engineered grafts are made from ESC-derived or iPSC–derived cardiomyocytes that may be immature, we next investigated whether neonatal CTS may be more resistant to ischemia, leading to better survival than adult CTS. Neonatal CTS (from 1-day-old pups) were transplanted onto adult control or infarcted hearts (Figure IIIC and IIID in the online-only Data Supplement). Although the BLI signal differed initially, overall cell survival was similar between the control and infarcted groups from day 7 onward (control versus infarct; *P*=0.63). One month after transplantation of 400-μm-thick neonatal CTS 35±6% of transplanted cells remained viable. This suggests a high ischemia resistance of neonatal CTS, because we found a 50% lower BLI signal intensity when adult CTS were transplanted onto infarcted hearts compared with control hearts. High ischemia resistance of neonatal cardiomyocytes has been reported previously corroborating our results.[16]

Histological Assessment and Confirmation of CTS Viability

Histologically, we observed heterogeneous green fluorescent protein expression in cardiac tissue from L2G mice (Figure 2). Because luciferase is expressed from the same promoter, we verified that viability can be measured by BLI. We found a linear relationship between CTS thickness and BLI signal intensity (r=0.97; P=4.95E-06; Figure IVA in the online-only Data Supplement). Similar to BLI survival data, most cell death occurred within a week after transplantation when assessed with terminal deoxynucleotidyl transferase mediated dUTP nick-end labeling assay (TUNEL) (Figure IVB in the online-only Data Supplement). To verify whether cell survival is diffusion limited and if there are differences in the survival rates of cardiac cell types, we performed TUNEL staining for cellular apoptosis. One day after CTS transplantation, a few apoptotic cardiac troponin T (cTnT)-expressing cardiomyocytes were found in the graft, whereas more dying platelet-endothelial cell adhesion molecule 1 (CD31)-positive endothelial cells and fibroblast specific protein 1 (FSP1)–positive cells were observed (Figure 2A–2C; Figure VA–VC in the online-only Data Supplement). Cell death increased on day 3 (Figure 2D–2F; Figure VD–VF in the online-only Data Supplement) and declined from day 6 to day 9 (Figure 2G-2L; Figure VG-VL in the online-only Data Supplement). On days 3 and 6, cell death increased with radial distance from the heart, again indicative of diffusion-limited cell survival. We observed a rapid decline in the number of cardiomyocytes and endothelial cells in the graft for the first 6 days after transplantation (Figure 2M and 2N). In contrast, the number of $FSP1^+$ cells increased, despite the high level of apoptosis in $FSP1^+$ cells (Figure 2O). Because macrophages have been reported to express FSP1,[17] tissue sections were stained for the pan-leukocyte marker CD45 (Figure VI in the online-only Data Supplement) to determine whether this increase reflects an influx of macrophages or other inflammatory cells. Although a small number of $CD45^+$ and CD45/FSP1 double-positive cells was found in normal myocardium (Figure VIA–VIC in the online-only Data Supplement), their number increased from the first day onward in the transplanted graft (Figure VID-–VIL in the online-only Data Supplement). On day 3, almost all $FSP1^+$ cells were $CD45^+$, indicating that the increase in FSP1-expressing cells was due to an influx of pan-leukocytic cells, likely macrophages. Later time points showed an increase in fibroblasts and a decrease in $CD45^+$ cells (Figure VIM–VIP in the online-only Data Supplement). To further verify that $FSP1^+$ cells are primarily from the host, CTS from adult Sox2-Cre; Rosa26-tdTomato double-heterozygous mice with permanent labeling of cells by tdTomato were transplanted onto the hearts of immunocompromised mice. Similar to L2G CTS transplantation, we found an increase in $FSP1^+$ cells from day 3 onward, most of which were tdTomato negative indicating host origin (Figure VII in the online-only Data Supplement).

Rapid Revascularization of Transplanted CTS

Revascularization of transplanted CTS is likely an important factor determining graft survival, particularly for increased thicknesses. Pre-existing vascular networks in CTS may favor their survival. Because CTS are made from normal myocardium with a pre-existing vasculature ($CD31^+$; Figure 3A), we aimed to investigate whether and when these vessels connect to the host vasculature following transplantation. Intravenous injection of lectins before euthanizing host animals efficiently labeled the host vasculature. One day after CTS

transplantation graft vessels were lectin negative (Figure 3A–3C). In contrast, 3 days after CTS transplantation, 68±12% of the graft vessels were lectin positive, indicating reperfusion (Figure 3D–3F; Figure VIII in the online-only Data Supplement). Similar results were obtained for day 6 (Figure 3G–3I). Although reperfused vessels were more homogeneously distributed from day 3 onward, the number of reperfused vessels did not increase and the vascular density decreased (Figure 3J). Importantly, we detected perfused vessels apparently connecting host and graft vasculature (Figure 3K–3M). To determine the origin of vessels connecting host and graft, CTS were transplanted onto noninfarcted hearts of adult VE-cadherin-Cre; Rosa26-tdTomato double-heterozygous mice with permanent labeling of host endothelial cells with tdTomato. After 2 weeks, tdTomato-positive vessels were found in the graft (Figure 4), indicating vessel invasion from the host. We found examples of host vessels connecting with graft vessels indicating anastomosis (Figure 4C). Although the vasculature of most grafts was reconnected through the epicardium, some grafts showed vessel ingrowth from surrounding tissue (Figure IX in the online-only Data Supplement). Taken together, these findings suggest that transplanting tissue grafts containing vascular networks leads to fast reperfusion mediated by host vessels through invasion and connection with the graft vasculature.

Functional Benefits of CTS

To assess functional benefits of adult CTS, immunodeficient mice were subjected to MI and received no treatment (control, n=12), CTS (n=12), or skeletal muscle patches of equal size (n=11). We included a skeletal muscle patch group to account for mechanical effects of CTS transplantation that may influence remodeling (Figure 5A). To rule out immediate effects of tissue slice transplantation on scar formation, late gadolinium enhancement MRI was performed on day 1 after surgery, demonstrating no difference in scar size due to CTS or skeletal muscle patch transplantation compared with control (P=0.80; Figure 5B–5E; Figure XA–XC in the online-only Data Supplement). We also performed BLI on these animals to track graft survival of the luciferase-expressing tissue slices. BLI of the CTS group demonstrated a typical initial cell loss for the first week and stabilization thereafter, preserving 14±6% of transplanted cells. In contrast, in the animals receiving skeletal muscle patches, we observed no initial cell loss and detected proliferation between days 21 and 28 after transplantation (Figure 5L). However, the excellent survival of skeletal muscle patches was not reflected in animal morbidity, because 45% of mice died before the end of the study (5 of 11; P=0.001), whereas no animals were lost in either control or CTS groups (Figure 5M). This poor survival might be because of arrhythmias induced by transplanted skeletal muscle patches, similar to what has been observed in a clinical trial involving the injection of human skeletal myoblasts into the heart (MAGIC: Myoblast Autologous Grafting in Ischemic Cardiomyopathy).[18]

Reduced Dilative Remodeling on CTS Transplantation

To assess whether CTS or skeletal muscle patches reduce dilative remodeling and preserve ejection fractions, cardiac MRI was performed on days 1 and 28 after MI and CTS or muscle patch transplantation (Figure 5F–5K; Figure XD in the online-only Data Supplement). We found significantly increased end-diastolic and end-systolic volumes for the skeletal muscle patch group (P=0.02, P=0.04) compared with control and CTS (Figure 5N and 5O). Ejection

fractions were similar 1 day after the surgery with 38±3%, 38±2%, and 38±3% for control, CTS, and skeletal muscle patch groups, respectively. However, 1 month later, the CTS group showed a higher preserved ejection fraction with 28±2% compared with control 21±2% and skeletal muscle patch group 19±3% (P=0.05; Figure 5P; Table I in the online-only Data Supplement). A similar trend was observed for cardiac output with the highest increase in the CTS group (Figure 5Q). Furthermore, a positive correlation between BLI signal intensity and ejection fraction (r=0.73; P=0.02) was observed in the CTS group on day 28, indicating that better cell survival leads to higher preserved ejection fraction. Conversely, a negative correlation was found for skeletal muscle patches (r=−0.90; P=0.01; Figure 5R and 5S).

Quantification of Cellular Composition of CTS

Because changes in graft composition after transplantation influence functional effects of these grafts on recipient hearts, we assessed graft composition 1 month after transplantation onto infarcted hearts. Control animals did not receive any grafts (Figure 6A–6C). CTS grafts derived from adult mice contained a small amount of cardiomyocytes (2±1%), endothelial cells (11±2%), and a high number of fibroblasts (24±7%) and $CD45^+$ cells (27±4%; Figure 6E–6H). We did not observe any obvious differences in size or composition of the scar tissue between the different groups (Figure 6). In contrast to the poor survival of cardiomyocytes in adult CTS, neonatal CTS contained a substantial number of cardiomyocytes (20±4%; Figure 6D). These neonatal cardiomyocytes may be more ischemia resistant,[16] leading to comparable survival when transplanted onto control or infarcted hearts (Figure XIA and XIB in the online-only Data Supplement). Grafts from neonatal CTS on infarcted hearts contained a similar number of fibroblasts and $CD45^+$ cells compared with adult CTS (Figure 6D). In contrast, skeletal muscle patch grafts contained almost no fibroblasts (1±1%) and a smaller number of $CD45^+$ cells (13±3%; Figure 6I–6L).

Discussion

The use of cardiac cell transplantation may be hampered by the degree of cell survival after transplantation. Notably, survival is typically <1% one month after injection of single-cell suspensions.[4,17] In contrast, engineered tissues derived from multiple cell sources may provide a better environment for preservation of transplanted cells. Accordingly, CTS generated from the native mammalian heart with its natural cellular organization were used as a model system to explore the results of transplantation of normal tissues. Using this unique model, we found that CTS transplantation led to long-term engraftment of ≤30% and 14% of transplanted cells on control and infarcted hearts, respectively. A pre-existing vascular network in the transplanted grafts likely contributed to the exceptional survival by quickly establishing vascular connection and reperfusion with the host hearts within 3 days after transplantation. The sectioning process used to make CTS led to cell death along the cutting edges, which became important for sections with <100 μm thickness, but for thicker sections the number of apoptotic cells found 1 day after implantation was low.

Our study demonstrates that initial cell survival is diffusion limited, with the highest survival rates between 300 and 400 μm slice thickness. Although previous reports suggested

survival of even thicker tissue-engineered grafts in vivo,[10,19,20] those survival estimates were primarily based on graft thickness at time of tissue harvest or histological evaluation of selected slices. Our study used noninvasive reporter gene imaging that can assess the entire graft repetitively and longitudinally over time. These advantages allow for more accurate and quantitative assessment of tissue graft survival. Because CTS consist of adult tissue while most tissue-engineered grafts consist of isolated ESC- or iPSC–derived cells that are likely immature, we also assessed the survival of neonatal CTS. These grafts showed comparable cell survival between infarcted and control hearts, indicating a higher hypoxia tolerance in accordance with previously published data.[16] Even so, overall cell survival did not exceed 35% for 400-μm-thick neonatal CTS.

A question that remains to be addressed is what cell composition would be suitable for tissue-engineered grafts and whether there are survival differences between different cell types found in the heart. CTS consist of myocardial tissue that contains a substantial number of endothelial cells and fibroblasts as well as cardiomyocytes. The presence of endothelial cells is needed to enable fast reperfusion because addition of endothelial cells or prevascularization of grafts improves survival, but the time course for reperfusion of cardiac patches has not been established.[8,11] Here, we found that grafts were reperfused within 3 days after transplantation. Cell death had reached a maximum by then and declined thereafter. This points to the importance of reperfusion and may offer a potential to improve graft survival by reducing the reperfusion/vascularization time and improve ischemia resistance for the first few days after transplantation.

When we assessed graft composition 4 weeks after transplantation onto infarcted hearts, CTS grafts contained mainly fibroblasts, pan-leukocytic cells, and endothelial cells. We only found a small number of cardiomyocytes in adult CTS. In contrast, neonatal CTS retained a substantial amount of cardiomyocytes when transplanted onto infarcted hearts. Previous publications reported reduced fibrosis and good cardiomyocyte survival of transplanted engineered tissues,[8,10,21] which may be due to the assessment of grafts mainly at the infarct border zone. In contrast, we assessed the entire graft that had been transplanted over the scar of the recipient heart and rarely reached onto noninfarcted tissue.

Previous studies indicated that transplantation of tissue-engineered patches reduces infarct/scar size, implying a paracrine mechanism.[22-24] We measured scar size 1 day after MI using high-resolution late gadolinium enhancement MRI and found that CTS or skeletal muscle patches did not reduce the infarct size in a mouse MI model, which might be because of differences in the animal model or assessment time points. We found reduced dilative remodeling, leading to a higher preserved ejection fraction in the CTS group compared with control and skeletal muscle patch groups, in line with published data for tissue-engineered patches.[9,10,25,26] A skeletal muscle patch was included in our functional analysis to control for potential mechanical effects of transplanted tissue reducing remodeling. Interestingly, skeletal muscle patches did not show cell loss when transplanted onto infarcted hearts in contrast to single-cell transplantation.[4] Accordingly, hearts receiving skeletal muscle patches had a higher wall thickness compared with both control and CTS groups, but only the CTS group showed functional improvements, suggesting that increased wall thickness is not necessarily a predictor for improved cardiac function.[9,27] Corroborating these results, a

positive correlation between cell survival and ejection fraction at 4 weeks was found for CTS, whereas a negative correlation was found for skeletal muscle patches. Finally, we observed a higher mortality after skeletal muscle tissue transplantation that might be because of arrhythmia, as previously reported for a clinical trial involving transplantation of autologous skeletal myoblasts into the ischemic heart,[18] but further studies are needed to investigate the underlying mechanisms.

In conclusion, this study shows that CTS transplantation leads to long-term engraftment of transplanted cells on infarcted hearts and reduced dilative remodeling. For CTS with <400 μm thickness, we observed high cell survival that may be due to rapid revascularization between the host organ and graft tissue. However, for CTS with >400 μm thickness, we observed poor survival, presumably because diffusion could not sustain the graft before it was revascularized. Importantly, these findings call for further improvements in graft revascularization before the cardiac tissue engineering strategy can be used for larger animals or humans. Finally, continued use of CTS and molecular imaging technologies will undoubtedly help accelerate the advancement of cardiac tissue engineering.

Supplementary Material

Refer to Web version on PubMed Central for supplementary material.

Acknowledgments

We thank Laura J. Pisani from the Stanford Small Animal Imaging Facility and Kitty Lee from the Cell Science Imaging Facility for their help with MRI and confocal imaging. We thank Jarrett Rosenberg for help with statistical analysis.

Sources of Funding

This study was supported by Erwin Schrödinger fellowships from the Austrian Science Fund (J. Riegler, A. Gillich); NIH Progenitor Cell Biology Consortium grant NIH U01 HL099995 (A. Gillich); U01 HL099776, NIH R01 EB009689, Leducq Foundation, AHA Established Investigator Award, and California Institute of Regenerative Medicine TR3-05556 (J.C. Wu).

References

1. Clifford DM, Fisher SA, Brunskill SJ, Doree C, Mathur A, Watt S, Martin-Rendon E. Stem cell treatment for acute myocardial infarction. Cochrane Database Syst Rev. 2012; 2:CD006536. [PubMed: 22336818]
2. Burridge PW, Keller G, Gold JD, Wu JC. Production of de novo cardiomyocytes: human pluripotent stem cell differentiation and direct reprogramming. Cell Stem Cell. 2012; 10:16–28. [PubMed: 22226352]
3. Shiba Y, Fernandes S, Zhu WZ, Filice D, Muskheli V, Kim J, Palpant NJ, Gantz J, Moyes KW, Reinecke H, Van Biber B, Dardas T, Mignone JL, Izawa A, Hanna R, Viswanathan M, Gold JD, Kotlikoff MI, Sarvazyan N, Kay MW, Murry CE, Laflamme MA. Human ES-cell-derived cardiomyocytes electrically couple and suppress arrhythmias in injured hearts. Nature. 2012; 489:322–325. [PubMed: 22864415]
4. van der Bogt KE, Sheikh AY, Schrepfer S, Hoyt G, Cao F, Ransohoff KJ, Swijnenburg RJ, Pearl J, Lee A, Fischbein M, Contag CH, Robbins RC, Wu JC. Comparison of different adult stem cell types for treatment of myocardial ischemia. Circulation. 2008; 118(14 Suppl):S121–S129. [PubMed: 18824743]
5. Li Z, Wilson KD, Smith B, Kraft DL, Jia F, Huang M, Xie X, Robbins RC, Gambhir SS, Weissman IL, Wu JC. Functional and transcriptional characterization of human embryonic stem cell-derived

Europe PMC Funders Author Manuscripts

endothelial cells for treatment of myocardial infarction. PLoS One. 2009; 4:e8443. [PubMed: 20046878]

6. Ye L, Zimmermann WH, Garry DJ, Zhang J. Patching the heart: cardiac repair from within and outside. Circ Res. 2013; 113:922–932. [PubMed: 24030022]
7. Chachques JC, Trainini JC, Lago N, Cortes-Morichetti M, Schussler O, Carpentier A. Myocardial Assistance by Grafting a New Bioartificial Upgraded Myocardium (MAGNUM trial): clinical feasibility study. Ann Thorac Surg. 2008; 85:901–908. [PubMed: 18291168]
8. Sekine H, Shimizu T, Hobo K, Sekiya S, Yang J, Yamato M, Kurosawa H, Kobayashi E, Okano T. Endothelial cell coculture within tissue-engineered cardiomyocyte sheets enhances neovascularization and improves cardiac function of ischemic hearts. Circulation. 2008; 118(14 Suppl):S145–S152. [PubMed: 18824746]
9. Miyahara Y, Nagaya N, Kataoka M, Yanagawa B, Tanaka K, Hao H, Ishino K, Ishida H, Shimizu T, Kangawa K, Sano S, Okano T, Kitamura S, Mori H. Monolayered mesenchymal stem cells repair scarred myocardium after myocardial infarction. Nat Med. 2006; 12:459–465. [PubMed: 16582917]
10. Zimmermann WH, Melnychenko I, Wasmeier G, Didié M, Naito H, Nixdorff U, Hess A, Budinsky L, Brune K, Michaelis B, Dhein S, Schwoerer A, Ehmke H, Eschenhagen T. Engineered heart tissue grafts improve systolic and diastolic function in infarcted rat hearts. Nat Med. 2006; 12:452–458. [PubMed: 16582915]
11. Stevens KR, Kreutziger KL, Dupras SK, Korte FS, Regnier M, Muskheli V, Nourse MB, Bendixen K, Reinecke H, Murry CE. Physiological function and transplantation of scaffold-free and vascularized human cardiac muscle tissue. Proc Natl Acad Sci U S A. 2009; 106:16568–16573. [PubMed: 19805339]
12. Cao YA, Wagers AJ, Beilhack A, Dusich J, Bachmann MH, Negrin RS, Weissman IL, Contag CH. Shifting foci of hematopoiesis during reconstitution from single stem cells. Proc Natl Acad Sci U S A. 2004; 101:221–226. [PubMed: 14688412]
13. Madisen L, Zwingman TA, Sunkin SM, Oh SW, Zariwala HA, Gu H, Ng LL, Palmiter RD, Hawrylycz MJ, Jones AR, Lein ES, Zeng H. A robust and high-throughput Cre reporting and characterization system for the whole mouse brain. Nat Neurosci. 2010; 13:133–140. [PubMed: 20023653]
14. Alva JA, Zovein AC, Monvoisin A, Murphy T, Salazar A, Harvey NL, Carmeliet P, Iruela-Arispe ML. VE-Cadherin-Cre-recombinase transgenic mouse: a tool for lineage analysis and gene deletion in endothelial cells. Dev Dyn. 2006; 235:759–767. [PubMed: 16450386]
15. Hayashi S, Lewis P, Pevny L, McMahon AP. Efficient gene modulation in mouse epiblast using a Sox2Cre transgenic mouse strain. Mech Dev. 2002; 119(Suppl 1):S97–S101. [PubMed: 14516668]
16. Malhotra R, Brosius FC 3rd. Glucose uptake and glycolysis reduce hypoxia-induced apoptosis in cultured neonatal rat cardiac myocytes. J Biol Chem. 1999; 274:12567–12575. [PubMed: 10212235]
17. Pinto AR, Paolicelli R, Salimova E, Gospocic J, Slonimsky E, Bilbao-Cortes D, Godwin JW, Rosenthal NA. An abundant tissue macrophage population in the adult murine heart with a distinct alternatively-activated macrophage profile. PLoS One. 2012; 7:e36814. [PubMed: 22590615]
18. Menasché P, Alfieri O, Janssens S, McKenna W, Reichenspurner H, Trinquart L, Vilquin JT, Marolleau JP, Seymour B, Larghero J, Lake S, Chatellier G, Solomon S, Desnos M, Hagège AA. The Myoblast Autologous Grafting in Ischemic Cardiomyopathy (MAGIC) trial: first randomized placebo-controlled study of myoblast transplantation. Circulation. 2008; 117:1189–1200. [PubMed: 18285565]
19. Lesman A, Habib M, Caspi O, Gepstein A, Arbel G, Levenberg S, Gepstein L. Transplantation of a tissue-engineered human vascularized cardiac muscle. Tissue Eng Part A. 2010; 16:115–125. [PubMed: 19642856]
20. Kawamura M, Miyagawa S, Fukushima S, Saito A, Miki K, Ito E, Sougawa N, Kawamura T, Daimon T, Shimizu T, Okano T, Toda K, Sawa Y. Enhanced survival of transplanted human induced pluripotent stem cell-derived cardiomyocytes by the combination of cell sheets with the pedicled omental flap technique in a porcine heart. Circulation. 2013; 128(11 Suppl 1):S87–S94. [PubMed: 24030425]

21. Masumoto H, Matsuo T, Yamamizu K, Uosaki H, Narazaki G, Katayama S, Marui A, Shimizu T, Ikeda T, Okano T, Sakata R, Yamashita JK. Pluripotent stem cell-engineered cell sheets reassembled with defined cardiovascular populations ameliorate reduction in infarct heart function through cardiomyocyte-mediated neovascularization. Stem Cells. 2012; 30:1196–1205. [PubMed: 22438013]

22. Maureira P, Marie PY, Yu F, Poussier S, Liu Y, Groubatch F, Falanga A, Tran N. Repairing chronic myocardial infarction with autologous mesenchymal stem cells engineered tissue in rat promotes angiogenesis and limits ventricular remodeling. J Biomed Sci. 2012; 19:93. [PubMed: 23146158]

23. Wei HJ, Chen CH, Lee WY, Chiu I, Hwang SM, Lin WW, Huang CC, Yeh YC, Chang Y, Sung HW. Bioengineered cardiac patch constructed from multilayered mesenchymal stem cells for myocardial repair. Biomaterials. 2008; 29:3547–3556. [PubMed: 18538386]

24. Fujimoto KL, Miki T, Liu LJ, Hashizume R, Strom SC, Wagner WR, Keller BB, Tobita K. Naive rat amnion-derived cell transplantation improved left ventricular function and reduced myocardial scar of postinfarcted heart. Cell Transplant. 2009; 18:477–486. [PubMed: 19622235]

25. Dvir T, Kedem A, Ruvinov E, Levy O, Freeman I, Landa N, Holbova R, Feinberg MS, Dror S, Etzion Y, Leor J, Cohen S. Prevascularization of cardiac patch on the omentum improves its therapeutic outcome. Proc Natl Acad Sci U S A. 2009; 106:14990–14995. [PubMed: 19706385]

26. Leor J, Aboulafia-Etzion S, Dar A, Shapiro L, Barbash IM, Battler A, Granot Y, Cohen S. Bioengineered cardiac grafts: A new approach to repair the infarcted myocardium? Circulation. 2000; 102(19 Suppl 3):III56–III61. [PubMed: 11082363]

27. Fujimoto KL, Tobita K, Merryman WD, Guan J, Momoi N, Stolz DB, Sacks MS, Keller BB, Wagner WR. An elastic, biodegradable cardiac patch induces contractile smooth muscle and improves cardiac remodeling and function in subacute myocardial infarction. J Am Coll Cardiol. 2007; 49:2292–2300. [PubMed: 17560295]

Europe PMC Funders Author Manuscripts

Europe PMC Funders Author Manuscripts

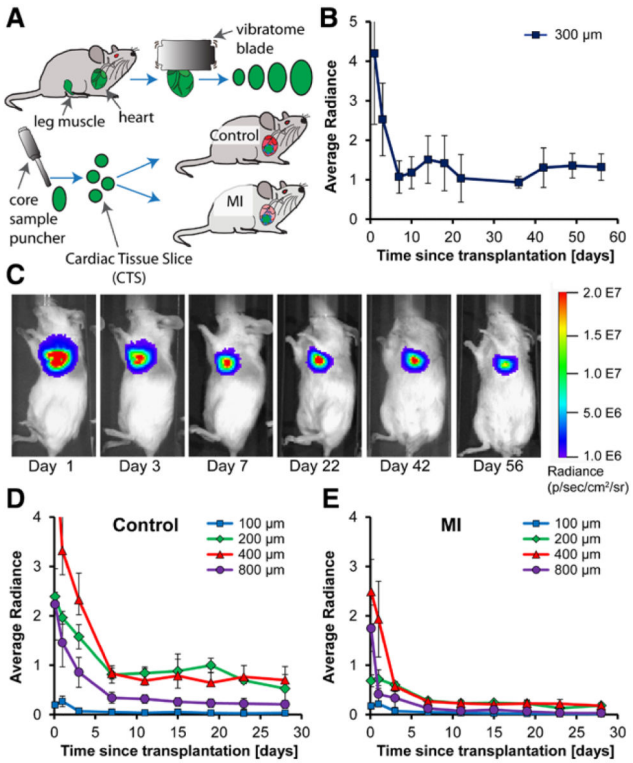

Figure 1.

Cardiac tissue slices show long-term engraftment with diffusion-limited survival during the first week supporting ≤400-µm-thick slices. **A**, Schematic illustration of cardiac tissue slice (CTS) generation and transplantation. **B** and **C**, CTS displayed bioluminescence imaging (BLI) signal loss for the first week with no further loss thereafter following transplantation into Nonobese Diabetic/Severe Combined Immunodeficiency (NOD/SCID) mice (n=4). **D**, The total amount of BLI signal per heart increased as the thickness of CTS was increased from 100 to 200 µm; a further increase to 400 µm or 800 µm led to decreased signal intensity (n=5 for each group). **E**, A similar pattern was observed for CTS transplanted onto infarcted hearts (n=5 for each group), but the overall signal was lower. Average radiance expressed as 10^6 photons/second per cm^2 per steradian. MI indicates myocardial infarction.

Europe PMC Funders Author Manuscripts

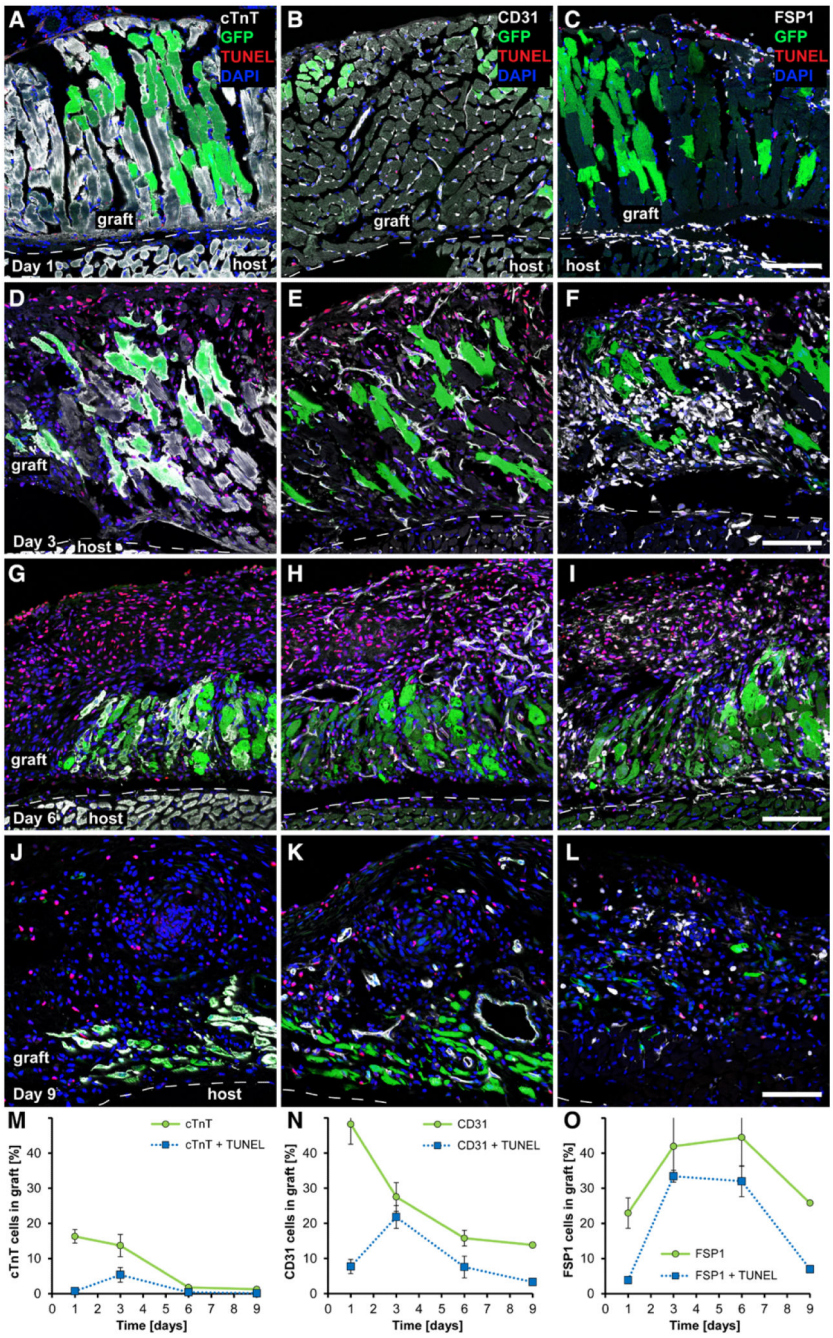

Figure 2.

Survival of cardiomyocytes, endothelial cells, and fibroblasts after cardiac tissue slice (CTS) transplantation in mice. **A** to **C**, A small number of apoptotic cells (TUNEL$^+$ nuclei, red) were distributed throughout the graft 1 day after CTS transplantation onto normal mouse hearts. **D** to **F**, Three days after transplantation, cell death was high at the edge of the graft and low in regions close to the heart. **G** to **I**, A similar pattern was observed at day 6. **J** to **L**, On day 9, only a small number of dead cells was found. **M** to **O**, Cell death peaked on day 3 for cardiomyocytes (cardiac troponin T [cTnT]), endothelial cells (CD31), and fibroblast

specific protein 1 (FSP1)–positive cells. The number of cardiomyocytes and endothelial cells decreased from day 3 onward, whereas the number of $FSP1^{+}$ cells increased despite a high rate of cell death, indicating cell proliferation or influx into the graft (n=3 for each time point). DAPI indicates 4′,6-diamidino-2-phenylindole (nuclei); GFP, green fluorescent protein (graft); and TUNEL, terminal deoxynucleotidyl transferase mediated dUTP nick-end labeling assay. Scale bars, 100 μm.

Europe PMC Funders Author Manuscripts

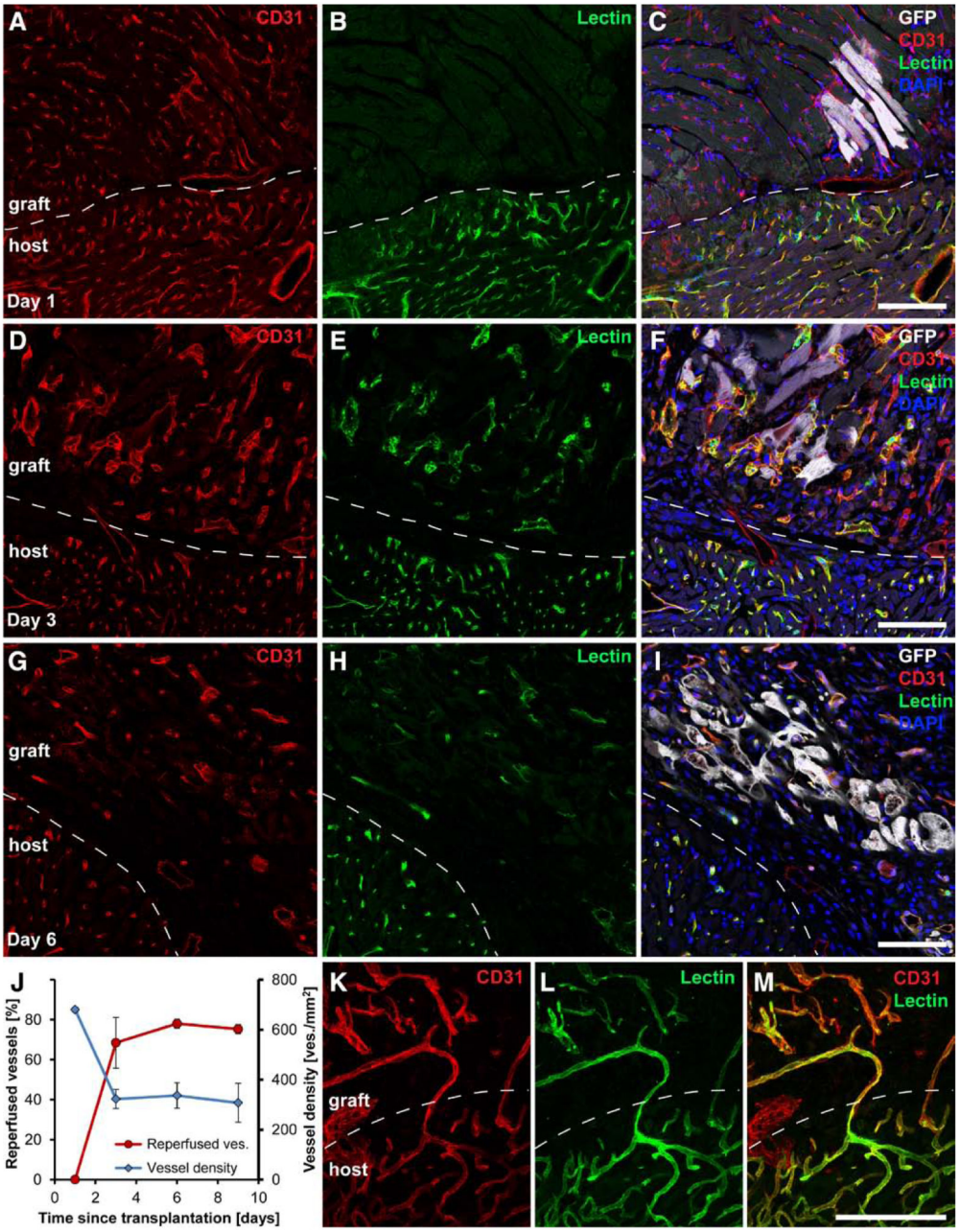

Figure 3.

Cardiac tissue slices are reperfused within 3 days after transplantation onto normal hearts. **A** to **C**, One day after transplantation, none of the graft vessels ($CD31^+$) were perfused (as shown by lack of detected signal after intravenous injection of biotinylated lectins) while host vessels were efficiently labeled. **D** to **F**, Three days later, a fraction of graft vessels was found to be perfused. **G** to **I**, The percentage of perfused vessels did not increase on day 6 or day 9. **J**, The vascular density declined from day 1 to day 3. **K** to **M**, Vessels connecting host and graft were readily detected (maximum intensity projection, day 3; n=3 for each time point). DAPI indicates 4′,6-diamidino-2-phenylindole (nuclei); and GFP, green fluorescent protein (graft). Scale bars, 100 μm.

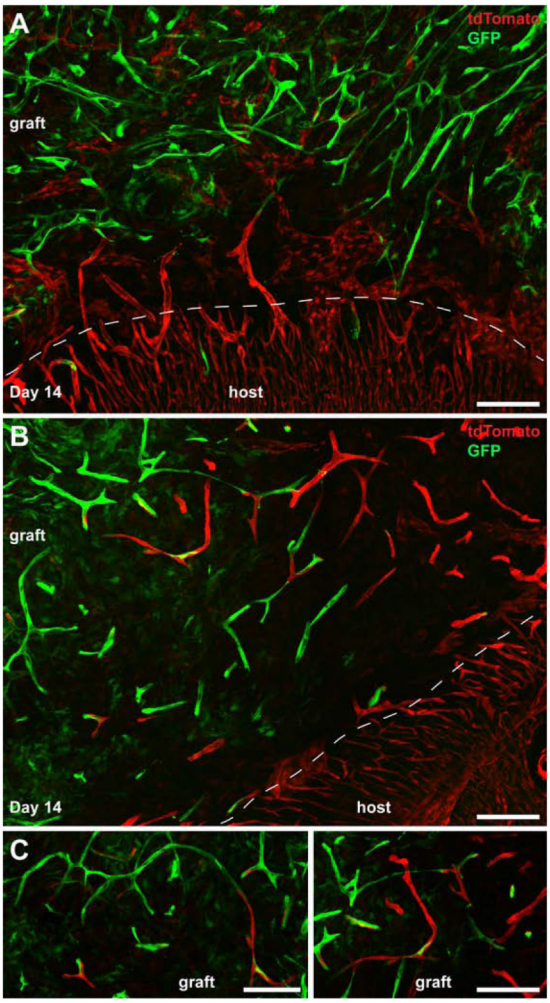

Figure 4.

Host vessels invade the cardiac tissue slices (CTS) and connect with the graft vasculature. CTS expressing green fluorescent protein (GFP, green) were transplanted onto VE-cadherin-Cre; Rosa26-tdTomato double-heterozygous hearts with permanent labeling of endothelial cells with tdTomato (red). **A** and **B**, The presence of tdTomato-labeled vessels in grafts at 14 days after transplantation indicates ingrowth of host-derived vessels. **C**, Examples for host vessels (red) connecting with graft vessels (green) indicative of anastomosis (n=3). Scale bars, 100 μm.

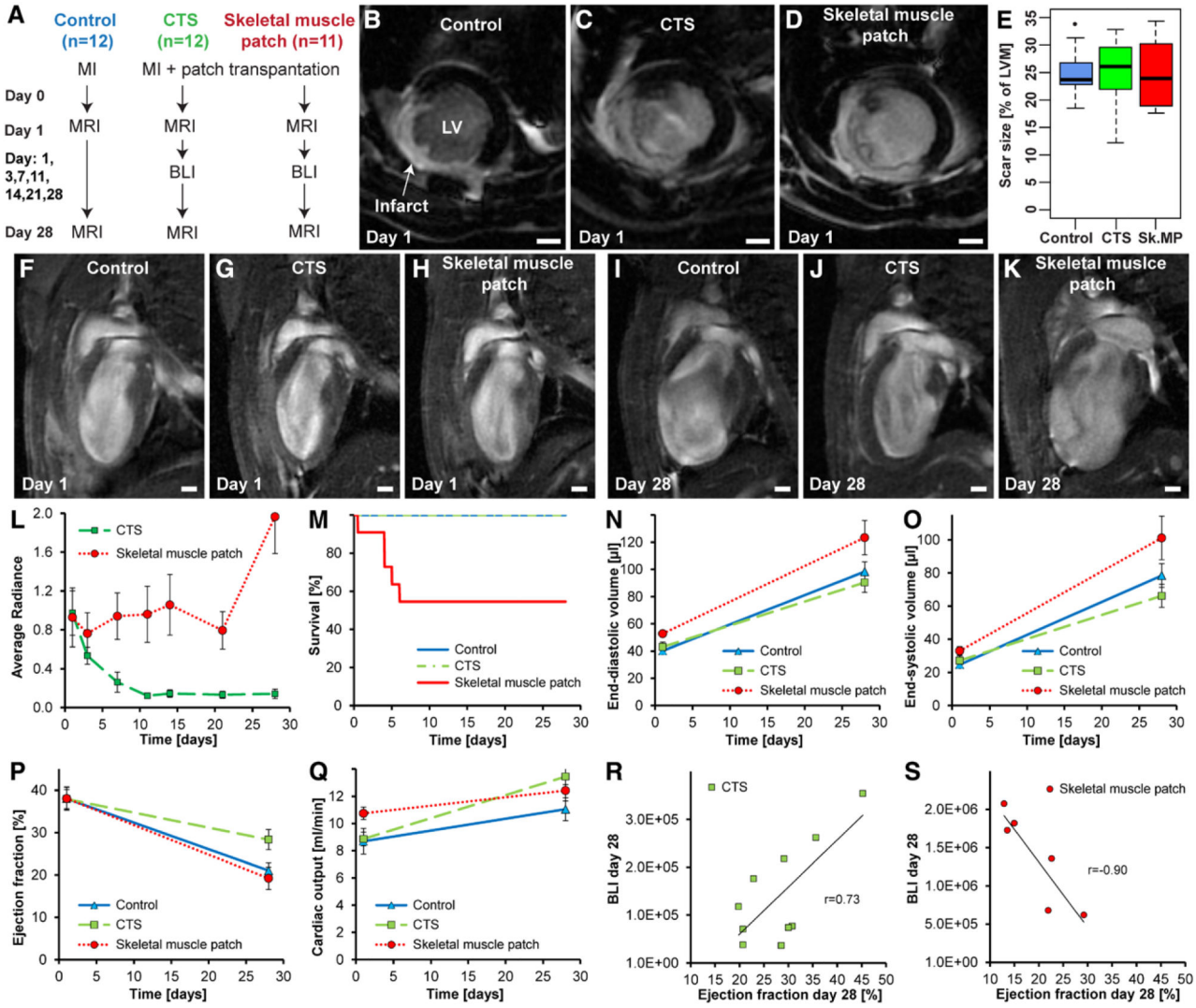

Figure 5.

Cardiac tissue slice (CTS) transplantation onto infarcted hearts improved cardiac function compared with control and skeletal muscle patches. **A**, Schematic overview of MRI and bioluminescence imaging (BLI) experiments for functional characterization. **B** to **E**, Representative midventricular short-axis late gadolinium enhancement MRI images showing that CTS or skeletal muscle patch transplantation did not alter the infarct size (scar size), which is expressed as percentage of the left ventricular mass (LVM). The boxplot for the control group in **E** contains a data point above the whisker, which is a potential outlier. **F** to **K**, Representative 2-chamber long-axis views illustrate dilative remodeling between days 1 and 28 in mice receiving no treatment: control (n=12), CTS (n=12), or skeletal muscle patch transplants (n=11). **L**, BLI demonstrated cell loss during the first 10 days after CTS transplantation (dashed green line) with no further cell loss thereafter. In contrast, skeletal muscle patches showed no cell death but cell proliferation between days 24 and 28 (dotted red line). **M**, Whereas no animal death occurred in the control (blue line) and CTS groups (dashed green line), 45% of the mice (5 of 11) in the skeletal muscle patch group died within

1 month after transplantation (red line). **N** and **O**, End-diastolic and end-systolic volumes increased faster in the skeletal muscle patch group compared with control and CTS. **P**, Ejection fractions were similar 1 day after surgery; 1 month later, the CTS group had a higher ejection fraction compared with control and skeletal muscle patch groups. **Q**, In line with that, cardiac output was highest in the CTS group. **R** and **S**, A positive correlation between cell survival on day 28 and cardiac function was observed for the CTS group (r=0.73; P=0.02), whereas a negative correlation was found for the skeletal muscle patch group (r=−0.90; P=0.01). MI indicates myocardial infarction; and Sk.MP, skeletal muscle patch. Scale bars, 1 mm.

Europe PMC Funders Author Manuscripts

Europe PMC Funders Author Manuscripts

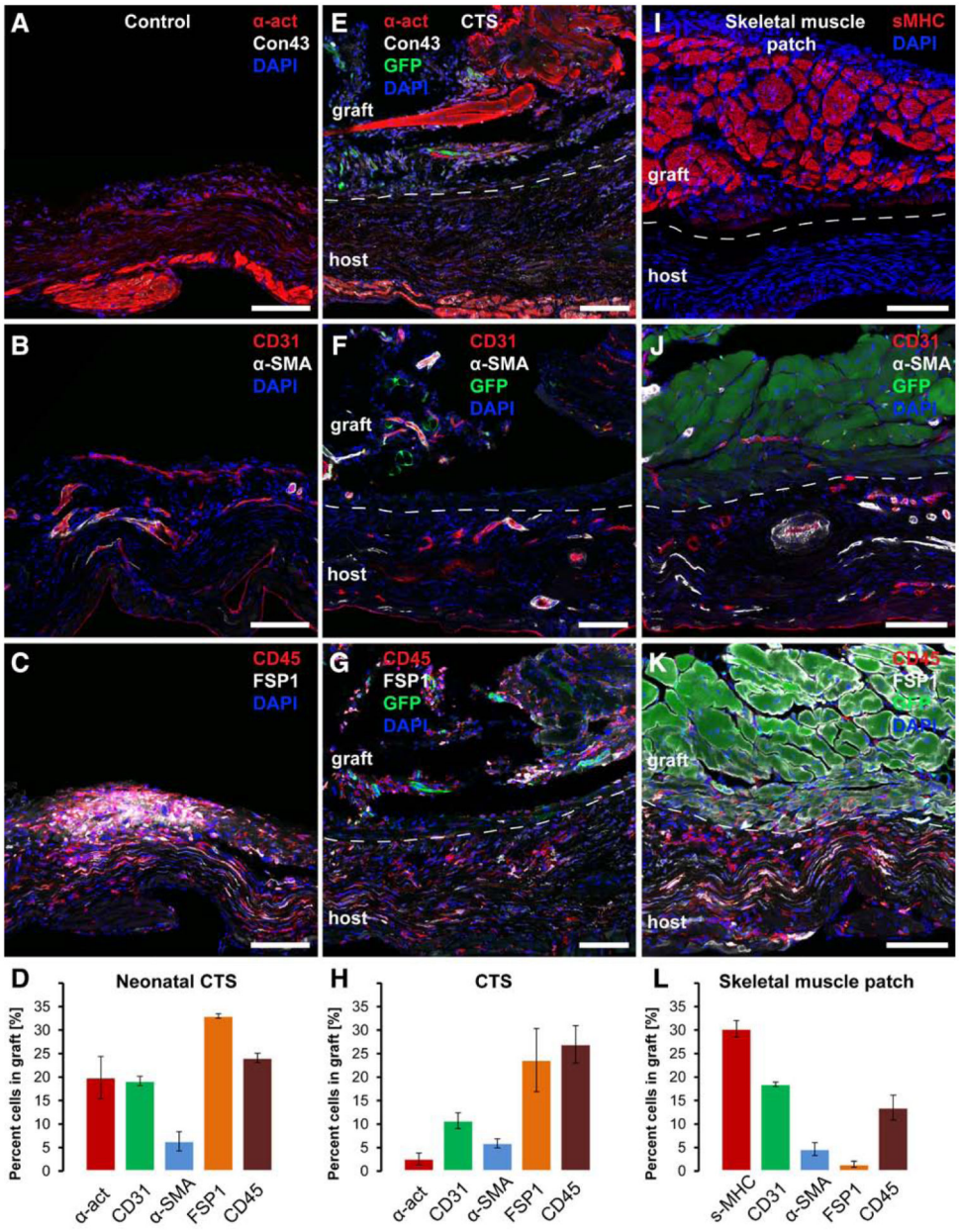

Figure 6.

Composition of cardiac tissue slices (CTS) and skeletal muscle patches 1 month after transplantation onto infarcted hearts. **A** to **C**, Control heart scar tissue contained a small number of surviving cardiomyocytes (α-actinin [α-act]) along the endocardial boarder, some blood vessels (CD31), and a high number of fibroblasts (fibroblast specific protein 1 [FSP1]) as well as CD45-positive cells. **D**, Neonatal CTS contained a high number of cardiomyocytes and endothelial cells and a substantial number of fibroblasts and $CD45^+$ cells. **E** to **H**, Adult CTS grafts contained a small number of cardiomyocytes, blood vessels, and a large number of fibroblasts and $CD45^+$ cells. **I** to **L**, Skeletal muscle patch grafts consisted primarily of myoblasts (skeletal myosin heavy chain [sMHC]) and endothelial cells. There were some $CD45^+$ cells and almost no fibroblasts in these grafts (n=4 per

group). αSMA indicates α-smooth muscle actin; Con43, Connexin 43; DAPI, 4′,6-diamidino-2-phenylindole (nuclei); and GFP, green fluorescent protein (graft). Scale bars, 100 μm.

Europe PMC Funders Author Manuscripts